JARO 11: 657–673 (2010)
DOI: 10.1007/s10162-010-0223-6

JARO
Journal of the Association for Research in Otolaryngology

Envelope Coding in Auditory Nerve Fibers Following Noise-Induced Hearing Loss

Sushrut Kale[1] and Michael G. Heinz[1,2]

[1]*Weldon School of Biomedical Engineering, Purdue University, 500 Oval Drive, West Lafayette, IN 47907, USA*
[2]*Department of Speech, Language, and Hearing Sciences, Purdue University, West Lafayette, IN 47907, USA*

Received: 12 January 2010; Accepted: 25 May 2010; Online publication: 16 June 2010

ABSTRACT

Recent perceptual studies suggest that listeners with sensorineural hearing loss (SNHL) have a reduced ability to use temporal fine-structure cues, whereas the effects of SNHL on temporal envelope cues are generally thought to be minimal. Several perceptual studies suggest that envelope coding may actually be enhanced following SNHL and that this effect may actually degrade listening in modulated maskers (e.g., competing talkers). The present study examined physiological effects of SNHL on envelope coding in auditory nerve (AN) fibers in relation to fine-structure coding. Responses were compared between anesthetized chinchillas with normal hearing and those with a mild–moderate noise-induced hearing loss. Temporal envelope coding of narrowband-modulated stimuli (sinusoidally amplitude-modulated tones and single-formant stimuli) was quantified with several neural metrics. The relative strength of envelope and fine-structure coding was compared using shuffled correlogram analyses. On average, the strength of envelope coding was enhanced in noise-exposed AN fibers. A high degree of enhanced envelope coding was observed in AN fibers with high thresholds and very steep rate-level functions, which were likely associated with severe outer and inner hair cell damage. Degradation in fine-structure coding was observed in that the transition between AN fibers coding primarily fine structure or envelope occurred at lower characteristic frequencies following SNHL. This relative fine-structure degradation occurred despite no degradation in the fundamental ability of AN fibers to encode fine structure and did not depend on reduced frequency selectivity. Overall, these data suggest the need to consider the relative effects of SNHL on envelope and fine-structure coding in evaluating perceptual deficits in temporal processing of complex stimuli.

Keywords: temporal coding, sensorineural hearing loss, phase locking, modulation coding

INTRODUCTION

Listeners with sensorineural hearing loss (SNHL) have difficulty understanding speech in fluctuating background noises (Duquesnoy 1983; Festen and Plomp 1990); however, neural correlates for this significant perceptual deficit remain unknown. Recent perceptual studies focused on temporal coding have suggested that envelope cues are most salient for understanding speech in quiet (Shannon et al. 1995) and fine-structure cues are most important for speech in noise (Qin and Oxenham 2003; Zeng et al. 2005). Listeners with SNHL appear to have reduced ability to use fine-structure cues for both speech and non-speech stimuli (Buss et al. 2004; Lorenzi et al. 2006; Hopkins and Moore 2007), and this deficit does not depend on reduced frequency selectivity (Lorenzi et al. 2009; Strelcyk and Dau 2009). In contrast, envelope coding is generally believed to be unaffected by SNHL. Hearing-impaired listeners often show near-normal ability to detect simple and complex patterns of amplitude modulation (Bacon and Gleitman 1992; Moore and Glasberg 2001; Sek and Moore 2006) and to perceive envelope-vocoded speech with minimal

Correspondence to: Sushrut Kale · Weldon School of Biomedical Engineering · Purdue University · 500 Oval Drive, West Lafayette, IN 47907, USA. Telephone: +1-765-4962613; fax: +1-765-4940771; email: skale@purdue.edu

spectral information (Baskent 2006; also see Lorenzi et al. 2006). However, several perceptual studies suggest that envelope coding is enhanced following SNHL and that this *enhancement* could produce a perceptual *deficit* for listening in complex backgrounds with fluctuating maskers (Moore et al. 1996; Fullgrabe et al. 2003). Loss of cochlear compression following outer hair cell damage was hypothesized to underlie this enhanced envelope coding; however, this hypothesis has not been tested physiologically. Considering that the influence of cochlear compression on hearing-impaired auditory nerve (AN) responses is limited by saturation and inner hair cell damage, it is not clear whether neural envelope coding would be affected by SNHL (Heinz et al. 2005).

The ability of AN fibers to phase lock to stimulus fine structure up to several kilohertz and to stimulus envelope for all carrier frequencies has been well characterized in normal-hearing animals (Johnson 1980; Joris and Yin 1992); however, very few studies have examined the effect of SNHL on fundamental aspects of temporal coding. Several studies suggest that SNHL does not affect the strength of AN fiber phase locking to tones (Harrison and Evans 1979; Miller et al. 1997); however, contradictory evidence does exist (Woolf et al. 1981). Another physiological factor that might affect envelope coding following SNHL is the presence of very steep rate-level functions in cases of moderate–severe threshold shifts. This steep response growth at high sound levels has been associated with so-called component-2 (C2) responses that are invulnerable to severe acoustic trauma. The C2 responses can be quite prominent when significant outer and inner hair cell stereocilia damage occurs (Liberman and Kiang 1984). Although these high-level irregularities are often ignored for normal hearing, they occur at sound levels (80–90 dB sound pressure level (SPL)) that are significant for hearing-impaired listeners using hearing aids and thus have important implications for level and speech coding (Heinz and Young 2004; Zilany and Bruce 2007).

The primary goal of the present study was to characterize effects of noise-induced hearing loss on the fundamental ability of AN fibers to phase lock to stimulus envelope. In addition, shuffled correlogram analyses were used to evaluate effects of SNHL on the relative strength of fine-structure and envelope coding (Joris 2003; Louage et al. 2004).

METHODS

Single-fiber AN recordings were made from nine normal-hearing and 11 hearing-impaired chinchillas, all males weighing between 400 and 650 g. All animal care and use procedures were approved by Purdue Animal Care and Use Committee.

Acoustic trauma

Sensorineural hearing loss was induced with the same protocol used previously in cats (Miller et al. 1997; Heinz and Young 2004), and for which anatomical/physiological correlates of acoustic trauma have been characterized (Liberman 1984; Liberman and Dodds 1984a, b; Liberman and Kiang 1984). Animals were first anesthetized by xylazine (1–1.5 mg/kg im) followed by ketamine (50–65 mg/kg im). Atropine (0.1 mg/kg im) was given to control mucus secretions, and eye ointment was used to prevent drying of the eyes. Prior to each noise exposure, auditory-brainstem responses (ABRs) between the dorsal midline and bulla were measured using sub-dermal electrodes. Normal-hearing ABR thresholds were verified at 1, 2, 4, and 8 kHz. Animals were then exposed to a 50-Hz wide noise band centered at 2 kHz uninterrupted for 4 h, in a free-field environment. Noise levels were calibrated to be 114–115 dB SPL at the entrance to the ear canal. Animals were allowed to recover for ≥30 days, after which ABRs were measured again to determine threshold shift. An ABR threshold shift of at least 20 dB at 2 kHz was considered as an indication of sufficient SNHL (Ngan and May 2001). In only one case was a re-exposure required due to insufficient threshold shift (10 dB at 2 kHz and no loss at other frequencies tested). The same protocol was followed during the re-exposure.

Surgical procedures and neurophysiological recordings

Before physiological recording, animals were anesthetized with xylazine (1–1.5 mg/kg im) followed by ketamine (50–65 mg/kg im). Atropine (0.1 mg/kg im) was given to control mucus secretions. In most animals, a catheter was placed in the cephalic vein to allow intravenous injections of sodium pentobarbital (~7.5 mg/kg/h iv) as supplemental anesthetic doses to maintain the state of areflexia. In four animals, the supplementary doses of sodium pentobarbital were given in the intra-peritoneal cavity. Physiological saline (2–5 ml/h iv) and lactated Ringer's solution (20–30 ml/24 h) were given to prevent dehydration. A tracheotomy was performed to allow a low-resistance airway. The skin and muscles overlying the skull were reflected to expose the ear canals and bulla. The bulla was vented with a 30 cm long polyethylene tube to maintain the middle ear pressure (Guinan and Peake 1967). The animal's rectal temperature was maintained at 37°C using a feedback-controlled heating pad.

During the recordings, the animals were held in place with a stereotaxic apparatus. The AN was exposed using standard techniques (Kiang et al. 1965; Heinz and Young 2004). A craniotomy was made in the posterior fossa and the cerebellum was partially aspirated. The remainder of the cerebellum was retracted medially with small cotton pellets. AN fiber recordings were made with a 10–30 MΩ glass micropipette filled with 3 M NaCl. Electrodes were placed under visual control as close as possible to where the AN trunk exits the internal auditory meatus, and then advanced into the nerve using a mechanical hydraulic microdrive. The electrode signal was amplified (Dagan, Minneapolis, MN, USA) and filtered prior to timing the action potentials (with 10-μs resolution) based on a time–amplitude window discriminator (Bak Electronics, Mount Airy, MD, USA).

Recordings were made in an electrically shielded, double-walled sound-attenuating room (Industrial Acoustics Company, Bronx, NY, USA). Computer-controlled stimuli were delivered monaurally through a custom closed-field acoustic system, with dynamic speakers (DT-48, Beyer Dynamic, Farmingdale, NY, USA) connected to a hollow ear bar that was inserted into the right ear canal to allow delivery of calibrated acoustic stimuli near the tympanic membrane. The acoustic system was calibrated at the beginning of the experiment using a probe-tube microphone (ER-7C, Etymōtic, Elk Grove Village, IL, USA) that was placed within a few millimeters of the tympanic membrane. Synchronous presentation of acoustic stimuli and data recording was controlled by custom software running in MATLAB (The Mathworks, Natick, MA, USA) that was integrated with commercial hardware (Tucker-Davis Technologies, Alachua, FL, USA; National Instruments, Austin, TX, USA). Experiments generally lasted from 24 to 38 h and were terminated by a lethal dose of barbiturate (Euthasol).

Single fibers were isolated by advancing the electrode through the AN while playing a broadband noise search stimulus (about 20 dB re 20 μPa/√Hz for normal-hearing animals, and higher as needed for noise-exposed animals). The state of the cochlea was monitored by tracking fiber thresholds as a function of characteristic frequency (CF) over time and looking for abrupt increases above the minimum thresholds collected early in the experiment. Only one normal-hearing experiment showed elevated thresholds (and broadened tuning) over time. All data collected after the threshold elevations were excluded from data analysis.

Stimuli

Isolated fibers were characterized initially by an automated tuning curve algorithm, which tracked the minimum sound level required for a 50-ms tone to elicit at least one more spike than a subsequent 50-ms silence (Kiang et al. 1970; Chintanpalli and Heinz 2007). Fiber CF, threshold, and Q_{10} (ratio of CF to tuning curve bandwidth 10 dB above threshold) were estimated from the tuning curve. In impaired fibers with broad tuning, CF was chosen based on the steep high-frequency slope of the tuning curve, which provides a good estimate of pre-exposure CF (Liberman 1984). For some impaired fibers, tuning was extremely broad and the low-frequency edge of the tuning curve did not rise to more than 10 dB above threshold. In such cases, an under-estimate of the 10-dB bandwidth was taken as the bandwidth between the lowest frequency for which a threshold was measured and the frequency corresponding to 10 dB above threshold at CF. Computed values of Q_{10} in these cases thus represent overestimates and are labeled as such in relevant figures. A few impaired fibers had 'w-shaped' tuning curves with a remnant sharp tip and a sensitive tail responding to a broad range of frequencies (Liberman and Dodds 1984b). For such fibers the broadest bandwidth was always used to compute Q_{10} values.

Fibers were further characterized by measuring CF-tone rate-level functions and post-stimulus-time (PST) histograms. CF-tone rate-level functions were measured with sound level raised in 1-dB steps from ~0 dB SPL to ~100 dB SPL. Each sound level was presented only once. The stimulus duration was 50 ms followed by 200 ms of silence. Least-square fits were made to the CF-tone rate-level functions with a first-order polynomial over the range from 10% to 90% of the maximum driven rate (as in Heinz and Young 2004). Slopes of CF-tone rate-level functions computed from the least-square fits were used in later analyses. PST histograms were measured with 50-ms CF-tone bursts followed by 200 ms of silence, presented 300 times at 30 dB above the tuning curve threshold. Recordings were verified to be from AN (rather than cochlear nucleus) based on (1) the monopolar shape of the spike waveforms and (2) the latency of the PST histogram.

AN fibers were also characterized based on spontaneous rate (SR), which was typically estimated from the CF-tone rate-level function. SR was computed by averaging the number of spikes that occurred within the silence portion of stimulus presentations at the lowest 10 presentation levels (~1 dB SPL to ~10 dB SPL). If rate-level data were not collected, SR was estimated from the PST histogram by averaging the number of spikes that occurred in the silence portion of stimulus presentations. AN fibers were classified as high spontaneous rate (HSR) if SR≥18 spikes/s, medium spontaneous rate (MSR) if 1≤SR<18 spikes/s, and low spontaneous rate (LSR) if SR<1 spikes/s (Temchin et al. 2008). For most analyses, LSR and MSR fibers

were combined into a low-medium spontaneous rate (LMSR) group.

Following the basic characterization, stimuli were presented from a set of amplitude-modulated (AM) sounds until the fiber was lost. Stimuli were either sinusoidally amplitude-modulated (SAM, Fig. 1A) tones or single-formant stimuli (SFS, Fig. 1E). The effect of sound level on envelope coding was measured for SAM tones by varying stimulus level from 5–10 dB below fiber's threshold to 30–40 dB above fiber's threshold in 5 dB steps. Carrier frequency (*fc*) was equal to fiber CF, modulation frequency (*fm*) was 50 Hz, and modulation depth (*m*) was held constant at 1.0 (full modulation). Each SAM tone was 600 ms long and a new sound level was presented every 1,000 ms until 20–30 repetitions of all levels were obtained. For each fiber, the SAM tone best modulation level (BML) was determined as the sound level for which the highest degree of synchrony to *fm* was observed. The SFS were created similarly to previous studies (Wang and Sachs 1993), with fundamental frequency (*F*0) equal to 100 Hz, formant frequency equal to CF, and formant bandwidth (3 dB down) of 60 Hz. The difference in modulation rate between the SAM tones (50 Hz) and SFS (100 Hz) was not expected to affect the results. Both normal and noise-exposed chinchilla AN fibers encode these two modulation frequencies equally well, as indicated by measured temporal modulation transfer functions, for the CF=1–4 kHz range of interest (Kale and Heinz, unpublished observations). The effect of sound level on temporal coding of SFS was evaluated by varying stimulus level from fiber threshold to 40–50 dB above threshold in 5 dB steps. SFS duration was 700 ms, with a new sound level presented every 1,000 ms. The 20–30 repetitions collected for each template produced ~1,500 spikes per condition, which was sufficient for the temporal analyses of AM coding described below.

Analysis

Three different metrics were used to quantify envelope coding in responses to SAM tones and SFS. The first metric was synchronization index (*R*, or vector strength), which was computed from period histograms with 64 bins (Goldberg and Brown 1969). Synchronization index is a measure of phase locking of AN fibers to the stimulus envelope when computed relative to *fm* for SAM tones or to fundamental frequency *F*0 for SFS. A Rayleigh uniformity test ($p < 0.001$) was used to test for significant deviations of the period histogram from a uniform distribution along the unit circle, based on the Rayleigh statistics of the quantity $2nR^2$, where n is the number of spikes (Mardia and Jupp 2000).

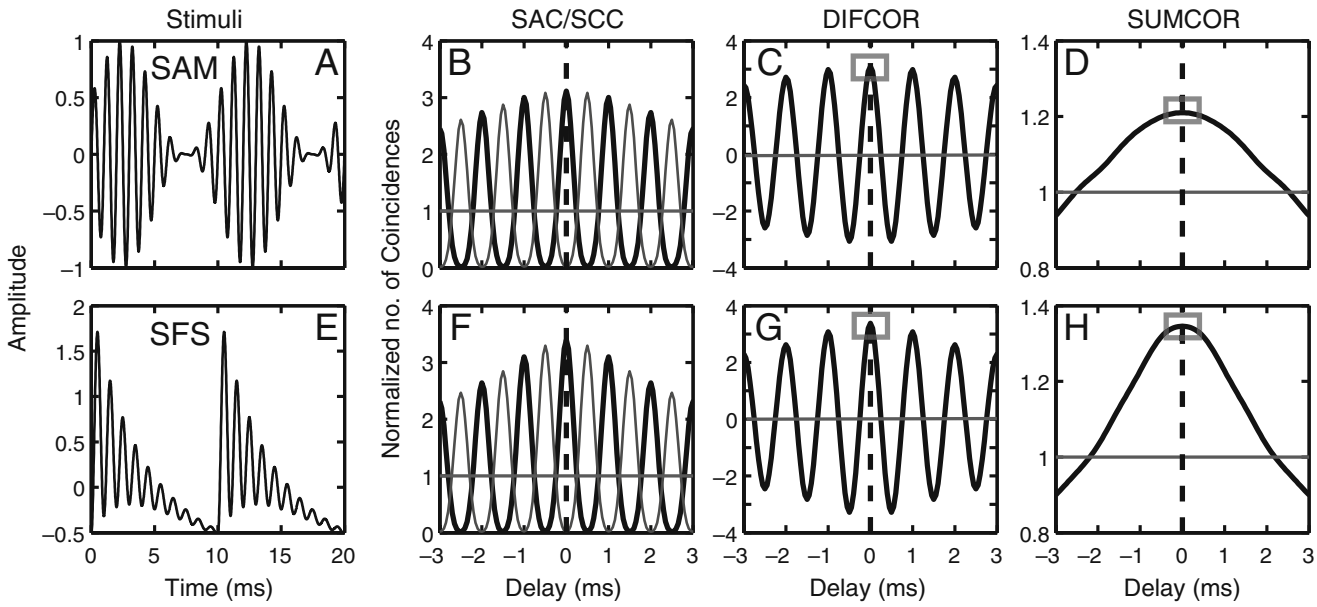

FIG. 1. Example time domain waveforms of amplitude-modulated stimuli used in this study and shuffled auto-correlogram (*SAC*) analysis metrics. **A–D** Sinusoidally amplitude-modulated (*SAM*) tones. **E–H** Single-formant stimuli (*SFS*). **A** and **E** Time domain waveforms. **B** and **F** *Thick black lines* show shuffled auto-correlograms [SACs (A+, A+)] and *thin gray lines* show shuffled cross-polarity correlograms [SCC (A+, A−)]. **C** and **G** Strength of fine-structure coding measured as difcor (SAC−SCC) peak height (*gray rectangles* in **C** and **G**). **D** and **H** Strength of envelope coding measured as sumcor [(SAC+SCC)/2] peak height (*gray rectangles* in **D** and **H**). For both SAM and SFS, carrier frequency was 1.5 kHz and stimuli were 100% modulated. SAM modulation frequency and SFS fundamental frequency were both 0.1 kHz for the examples shown, which permits better comparison between the correlograms; however, SAM modulation frequency was 50 Hz for all data reported in this study. *Horizontal gray lines* in correlogram panels indicate values corresponding to no correlation.

The second metric computed was response modulation [RM = (response envelope peak − response envelope valley)/response envelope peak]. Response modulation is a value that ranges from 0 to 1 and measures the modulation depth of the envelope of the period histogram (Wang and Sachs 1993). The envelope was computed using the fractional envelope technique based on the Hilbert transform, as described by Wang and Sachs (1993). Fractional envelopes are essentially the components of the Fourier transform of the period histogram with magnitude greater than an empirically determined noise floor (~20% of the dc component). The sum of fractional envelopes constitutes the true envelope of a period histogram (Wang and Sachs 1993). Period histograms used to compute RM included 256 bins based on *fm* for SAM tones and *F0* for SFS.

The third envelope metric computed was based on shuffled correlogram analyses, which allow for the separation of temporal envelope and fine-structure responses (Joris 2003). Shuffled auto-correlograms (SACs, thick black lines in Fig. 1B, F) were computed from a set of spike trains obtained in response to repeated presentations of a single stimulus (see Louage et al. 2004 for details). SACs were computed by tallying the intervals between all spikes across repetitions, rather than within repetitions. The shuffling across repetitions avoids the effects of refractoriness and provides a smoother representation of the temporal characteristics of the neural response than standard all-order interval histograms. SACs are analogous to auto-correlation functions, with similar properties such as a peak value at 0 delay and symmetry. Envelope and fine-structure components can be separated by comparing the responses to the stimulus and its polarity-inverted pair (Joris 2003; Louage et al. 2004). Polarity inversion does not affect the stimulus envelope, but inverts the stimulus fine structure. Shuffled cross-polarity correlograms [SCC(A+, A−), thin gray lines in Fig. 1B, F] were computed by tallying intervals between each spike in response to the original stimulus (A+) and each spike in response to the polarity-inverted stimulus (A−). The envelope component of the neural response can be emphasized by computing the average of the SAC(A) and SCC(A+, A−), which has been referred to as the sumcor (Joris 2003; Louage et al. 2004). Leakage of fine structure into the sumcor occurs for low CFs as an undesired spectral component centered at 2×CF due to rectification inherent in neural responses, but was eliminated by removing spectral components of the sumcor at frequencies above CF (Heinz and Swaminathan 2009). The strength of envelope coding was quantified as the peak height of the corrected sumcor for both SAM tone and SFS responses (Fig. 1D, H). The strength of fine-structure coding was likewise quantified from shuffled correlograms as the peak height of the difcor (Fig. 1C, G), which was computed as the difference between SAC(A) and SCC(A+, A−) (Joris 2003; Louage et al. 2004).

Because correlogram analyses were not planned from the outset of this study, responses were only measured to positive polarity SAM tones and SFS. However, the responses to negative polarity SAM tones can be approximated by shifting the measured spike times by one half of the carrier frequency period (Louage et al. 2004). To compute SCC(A+, A−) for SAM tones, half of the measured spike trains were shifted to create a second set of spike trains that approximates responses to the polarity-inverted (A−) SAM tone. To increase the number of spikes available to compute SACs and SCCs in each condition (~1,500 spikes are required for smooth correlograms), spike trains were combined across a 10-dB range of sound levels (i.e., three conditions, since SAM tone responses were measured in 5-dB steps). Thus, combining spikes across levels effectively represents a three-point moving average of the sumcor (or difcor) peak height versus level curve. Analysis of conditions for which enough spikes were available at each level confirmed that this three-point moving average led to a slight reduction in the maximum sumcor peak height. However, the similarity in the level dependence of envelope coding in normal-hearing and noise-exposed fibers (see Fig. 3) suggests that this slight underestimation of envelope coding due to three-point smoothing was similar between normal and impaired populations and thus did not influence the conclusions from this study.

RESULTS

Characterization of hearing loss

Hearing loss induced by acoustic trauma was characterized based on thresholds and Q_{10} values of individual AN fibers. Figure 2 shows the thresholds and Q_{10} values computed from the tuning curves of AN fibers obtained from normal-hearing animals (left column) and from animals with noise-induced hearing loss (NIHL, right column). Data shown in Figure 2 include 255 fibers pooled across nine normal-hearing animals (crosses) and 233 fibers pooled across 11 animals with NIHL (circles).

The solid lines in Figure 2A, B indicate the lowest thresholds observed in the normal-hearing (thin line) and noise-exposed (thick line) populations. These best-threshold curves are likely to better represent the behavioral audiogram than mean-threshold curves. Best thresholds were elevated in the NIHL population primarily between 1 and 8 kHz, with a ~35–40 dB shift for CFs between 2 and 3 kHz and only about a 10-dB shift for CFs below 1 kHz. This configuration of best threshold elevation is consistent with previous

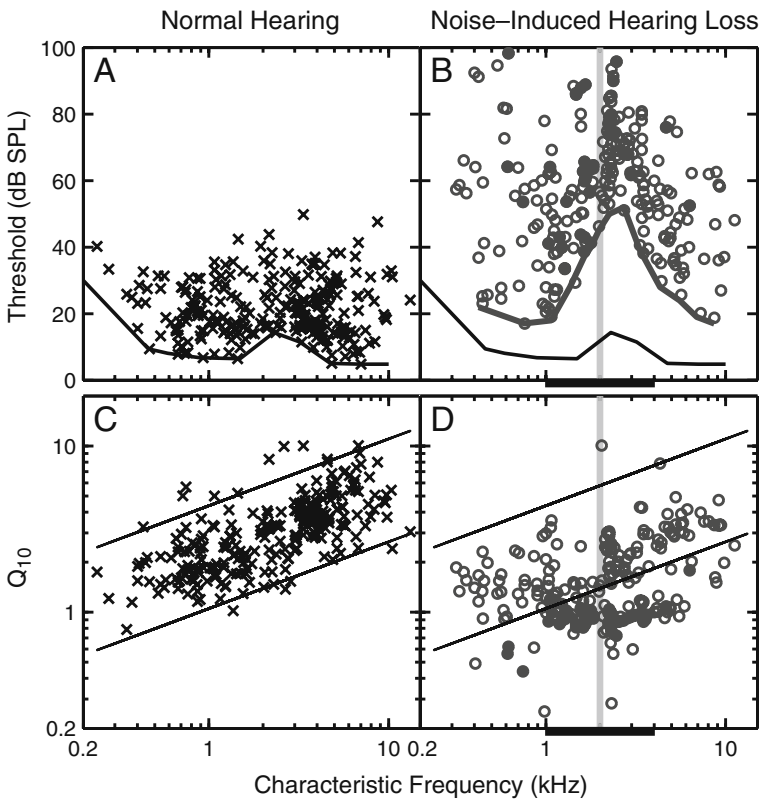

FIG. 2. Tuning curve characteristics as a function of characteristic frequency for the normal-hearing (*left*) and noise-induced hearing loss (*right*) populations. **A**, **B** Fiber thresholds at CF. *Solid lines* represent the distribution of best thresholds across CF (*thin* normal, *thick* impaired). **C**, **D** tuning curve sharpness as represented by Q_{10} (ratio of CF to bandwidth 10 dB above threshold). *Solid lines* represent the 5th and 95th percentiles of the normal-hearing population. **B** and **D** *Filled symbols* indicate AN fibers for which Q_{10} was overestimated (see text). The 50-Hz wide noise band used to induce hearing loss is indicated by the *shaded area*. *Thick horizontal bar* represents CF range (1–4 kHz) over which significant threshold shift occurred in all impaired fibers.

studies that used a similar noise band exposure (Miller et al. 1997; Heinz and Young 2004).

The thick bar along the abscissa indicates the ±1 octave CF region (1–4 kHz) surrounding the 2-kHz noise exposure frequency (vertical-shaded region). Quantitative comparisons between response properties of normal-hearing and noise-exposed fibers were made within this limited-CF region to reduce the influence of any CF dependencies, while ensuring that an adequate number of fibers were present in each population. In interpreting these comparisons, it is important to note that all noise-exposed fibers within this "impaired CF region" had significant threshold elevation; however, not all fibers with significant threshold elevation were within this limited-CF region.

Many individual AN fibers from the noise-exposed population had threshold elevations greater than the best-threshold shifts. Within the "impaired CF region", mean thresholds from the normal population were 18±7 dB SPL for HSR fibers and 27±9 dB SPL for LMSR fibers, consistent with previous chinchilla studies (Temchin et al. 2008). Mean thresholds for NIHL fibers were 52±16 dB SPL for HSR fibers and 65±19 dB SPL for LMSR fibers.

Figure 2C, D shows Q_{10} values of individual AN fibers as a function of CF. Solid diagonal lines represent the 5th and 95th percentile regions computed for the normal-hearing Q_{10} data (as in Bruce et al. 2003). Most noise-exposed fibers with CFs below 1 kHz and above 6 kHz had Q_{10} values within the normal range, suggesting little effect of noise exposure on frequency selectivity for CFs well away from the exposure frequency. Many fibers with CFs between 1 and 6 kHz had Q_{10} values that were below the 5th percentile for normal hearing, indicating a significant degradation in frequency selectivity in these fibers. However, note that a number of exposed fibers in this CF range had Q_{10} values within normal limits (albeit mostly within the lower half of the normal range). Impaired fibers for which Q_{10} was overestimated (i.e., for which extremely broad tuning made it difficult to estimate the 10-dB bandwidth, see Methods) are shown with filled symbols in Figure 2B, D. Frequency selectivity in these fibers is likely to be even worse than indicated by the filled circles.

In the normal-hearing population (N=255), 69% of the fibers were HSR, 25% were MSR, and 8% were LSR. The distribution of fibers across these three SR classes is consistent with previous data from normal-hearing chinchillas (Temchin et al. 2008). Within the CF range of 1–4 kHz, the distribution of fibers across the three SR classes was similar: 72% HSR, 22% MSR, and 6% LSR for the normal-hearing population (N=111). In the NIHL population, the distribution within the impaired CF region was 57% HSR, 25% MSR, and 19% LSR (N=120). The reduction in HSR fibers and increase in LSR fibers following NIHL is consistent

with previous acoustic trauma studies (Liberman and Dodds 1984a; Heinz and Young 2004).

Level dependence of modulation coding was not affected by noise-induced hearing loss

The non-monotonic level dependence of modulation coding that is a characteristic of normal-hearing fibers (Joris and Yin 1992; Wang and Sachs 1993) was also observed in all fibers from noise-exposed animals. Figure 3 shows rate- and synchrony-level functions for SAM tones (top row) and SFS (bottom row) for one normal-hearing (Fig. 3A, D) and two noise-exposed AN fibers (Fig. 3B, C, E, F). Phase locking to stimulus envelope begins to increase near rate threshold, peaks at a sound level (BML, see Methods) within the rate dynamic range, and then decreases well before rate begins to saturate as sound level increases further. This pattern was observed for all three envelope coding metrics considered, and was always similar between normal-hearing and noise-exposed fibers. In all NIHL fibers, synchrony-level functions were shifted to higher levels by the amount of the threshold shift. Many impaired fibers showed higher synchrony and steep SAM and SFS rate-level functions (e.g., Fig. 3C, F), as discussed in more detail below. The phase of individual components of SAM tones (*fm*, *fc*, and two side bands) generally remained unchanged with increasing sound level for both normal and noise-exposed fibers (not shown) over the range of levels for which responses were measured to characterize BML. While this level independence of SAM phase responses is generally consistent with previous normal-hearing studies, sharp phase transitions were reported in a few low-CF fibers at high sound levels (Joris and Yin 1992).

The dynamic range of modulation coding was quantified for each metric based on the range of sound levels over which the metric dropped to 90%, 75%, and 50% of the maximum (thin horizontal lines in Fig. 3). Dynamic range values corresponding to a drop to 75% of the maximum synchrony to SAM tones are shown in Figure 4A. The distributions of individual-fiber dynamic ranges overlapped within the impaired CF region (thick bars), with the mean and standard deviations being 23.5±3.0 dB for the normal-hearing population and 23.2±6.0 dB for the NIHL

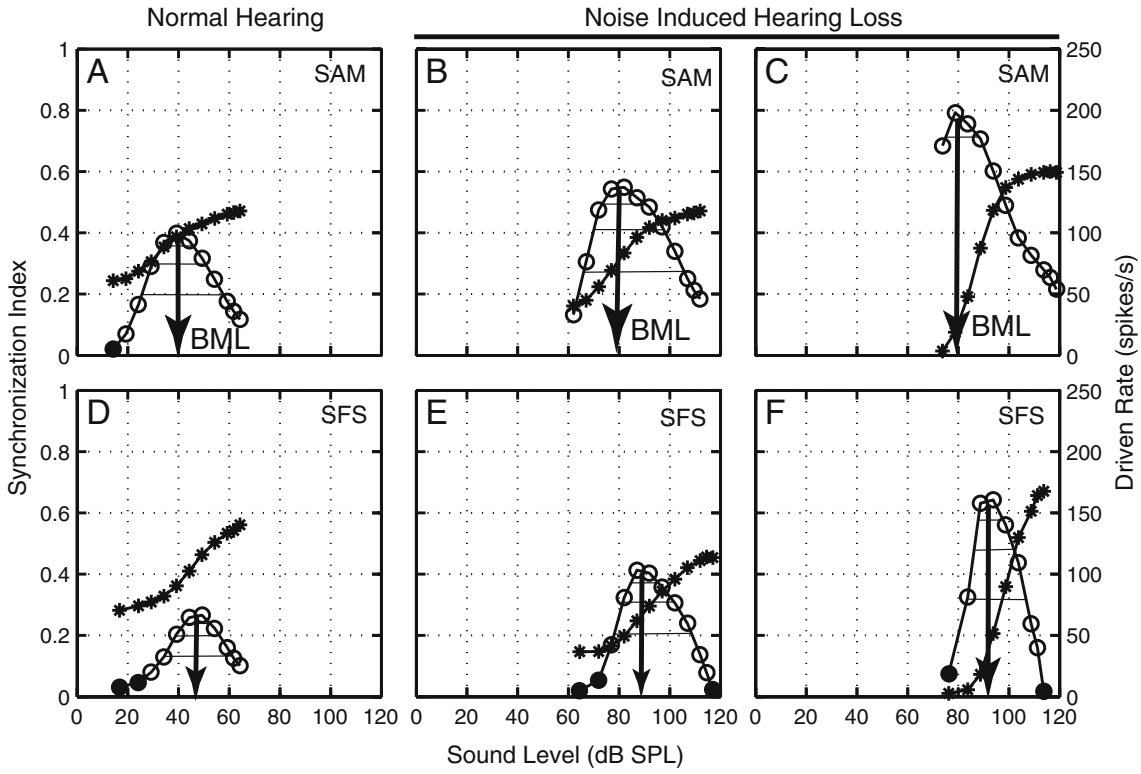

FIG. 3. The non-monotonic dependence of envelope coding on level was similar between normal-hearing (**A** and **D**) and noise-exposed (**B** and **C** and **E** and **F**) AN fibers for both SAM tones (*top row*) and SFS (*bottom row*). *Asterisks*: Driven rate as a function of sound level. *Circles*: Synchrony-level functions. *Filled symbols*: statistically (Rayleigh) insignificant synchronization index values. *Arrows*: Best modulation level (BML). *Solid horizontal lines*: dynamic range defined by envelope coding above 90%, 75%, and 50% of the maximum synchrony for each fiber and stimulus. In the third column, the noise-exposed fiber (**C** and **F**) has higher synchrony and a steeper rate-level function as compared to the other noise-exposed fiber (see text for details). Normal fiber (**A**, **D**): CF=2.10 kHz, threshold=13 dB SPL, Q_{10}=3.27, spontaneous rate (SR)=73 spikes/s; noise-exposed fiber (**B**, **E**): CF=2.35 kHz, threshold=63 dB SPL, Q_{10}=1.7, SR=48 spikes/s. Noise-exposed fiber with higher synchrony (**C**, **F**): CF=2.25 kHz, threshold=77 dB SPL, Q_{10}=0.8 and SR=5 spikes/s.

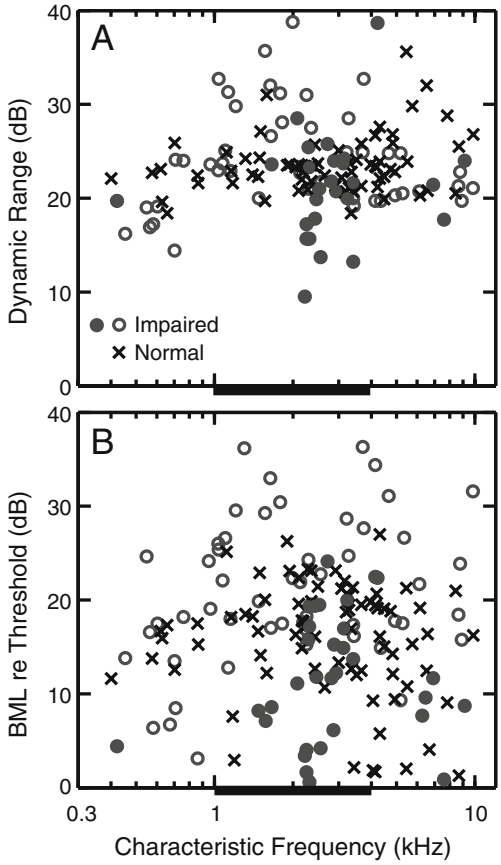

FIG. 4. The dynamic range of envelope coding was unaffected by noise-induced hearing loss. **A** Dynamic range of modulation coding above 75% of maximum synchrony coefficient for SAM tones (see Fig. 3). **B** Best modulation level (BML) relative to fiber's pure tone threshold. *Filled circles* represent impaired fibers with a high degree of enhanced envelope coding (see text). *Thick horizontal bar* represents CF region (1–4 kHz) of significant threshold shift.

population. A few noise-exposed fibers with CFs between 2 and 4 kHz had a smaller dynamic range than any of the normal-hearing fibers with similar CFs (Figs. 3F and 4A). Each of these fibers showed a high degree of envelope enhancement (defined quantitatively below) and had very steep rate-level functions, which would be expected to reduce the dynamic range for envelope coding. Except for the higher variability in dynamic range values for NIHL fibers, all three dynamic ranges (90%, 75%, and 50%) for synchrony-level functions were comparable between normal and NIHL populations. Similar results were obtained for all three envelope metrics and for both SAM tones and SFS (data not shown). The relative level difference between BML and pure tone rate threshold was also compared between normal-hearing and hearing-impaired populations for each metric. Figure 4B illustrates that this aspect of the level dependence of envelope coding was also not affected by NIHL. Similar results were obtained for all three envelope coding metrics and for SFS. Thus, the level dependence of envelope coding does not appear to be affected (beyond a threshold shift) by NIHL.

Envelope coding was enhanced following noise-induced hearing loss

Figure 5 compares envelope coding in the normal-hearing and noise-exposed populations. Each of the three envelope metrics (columns) is plotted as a function of CF for both SAM tones (top row) and SFS (bottom row). Each data point in Figure 5 is the maximum value of the metric computed at the BML (see Fig. 3), and thus these data provide a comparison between the best envelope coding in normal and noise-exposed fibers to these stimuli. There was no indication that envelope coding was degraded (lower metric values) in any noise-exposed AN fibers. In contrast, the trend lines for each metric indicate that envelope coding was enhanced on average following NIHL. This average enhancement occurred despite the substantial overlap between the normal and noise-exposed populations that arises due to the large variability in population data that is typical in AN responses. The enhancement in envelope coding occurred primarily within the CF region of significant threshold shifts (1–4 kHz). In this CF region, where all noise-exposed fibers showed clear threshold elevation (Fig. 2A), both the minimum and maximum values of each envelope metric were elevated in the impaired population relative to the normal population. The one exception was the response modulation metric (Fig. 5B), where the maximum value was saturated near 1.0 for both normal and impaired fibers. For CFs where there was less threshold shift (outside the 1–4 kHz range), the normal and noise-exposed populations essentially overlapped and thus there was less difference between the normal and impaired trend lines.

A group of noise-exposed fibers showed envelope coding metric values that were well above the range for all normal-hearing fibers with similar CFs. These fibers typically had CF values within the range of significant threshold elevation, and thus contributed to the average enhancement in envelope coding indicated by the trend lines. However, this subpopulation of noise-exposed fibers was not solely responsible for the average enhancement in envelope coding. The mean sumcor peak height for noise-exposed fibers computed after excluding fibers with sumcor peak height ≥ 2 was significantly higher than for normal-hearing fibers, as discussed in more detail below. This result suggests that most of the noise-exposed AN fibers with CFs in the range of significant threshold shifts had enhanced envelope coding following NIHL, with a subset of fibers showing a high degree of envelope enhancement. The data and

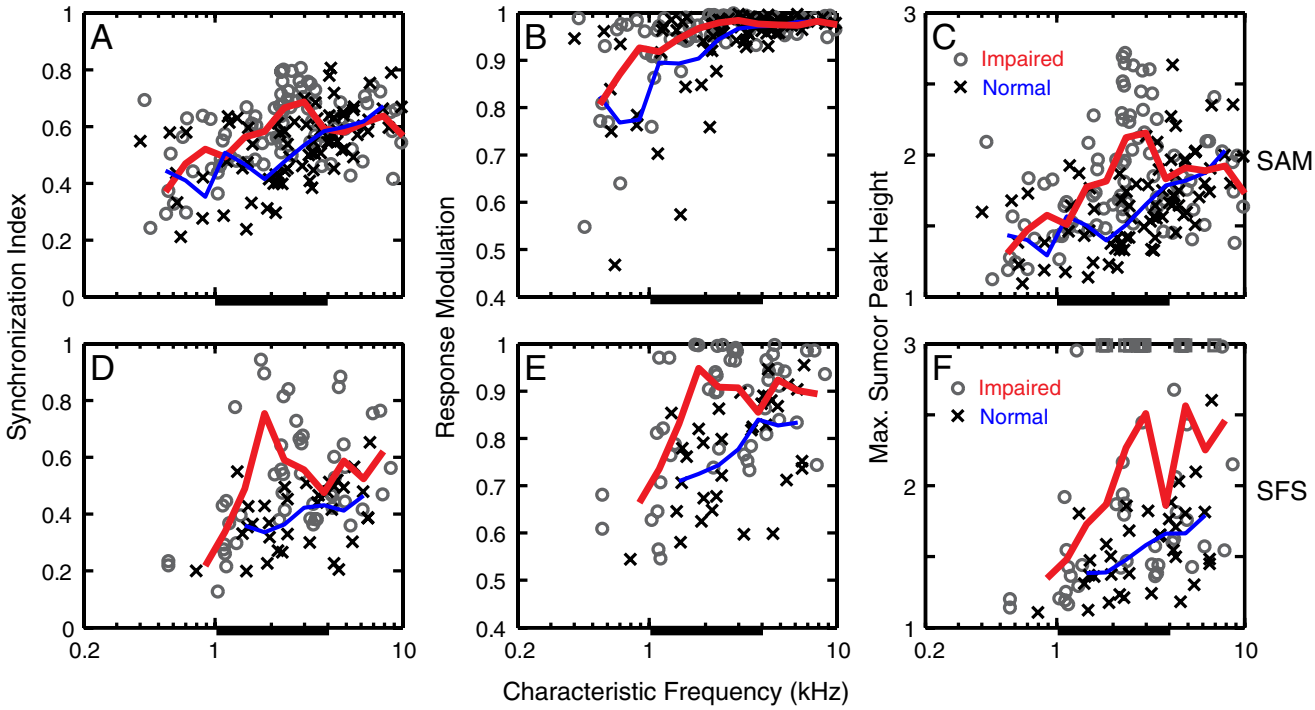

FIG. 5. Enhanced envelope coding was observed following noise-induced hearing loss based on all three envelope coding metrics. **A–C** Sinusoidally amplitude-modulated (*SAM*) tones. **D–F** Single-formant stimuli (*SFS*). Envelope coding metrics: (**A**, **D**) synchronization index, (**B**, **E**) response modulation depth, and (**C**, **F**) Sumcor peak height. Each data point is the maximum value of the corresponding metric computed at the best modulation level for that metric. *Crosses*: Normal hearing, *circles*: noise exposed. *Solid lines* (*thin*: normal hearing, *thick*: noise exposed) are triangular weighted averages across 0.7-octave wide windows (0.35-octave steps, at least four points in each window). *Thick horizontal bar* below each panel represents the CF region of significant threshold shifts (1 kHz≤CF≤4 kHz). Squares along the top *x*-axis in **F** indicate noise-exposed fibers with sumcor peak height >3.

trend lines also suggest that the degree of enhancement was greater for the more complex SFS (Fig. 5, bottom row) than for SAM tones (Fig. 5, top row). For example, the maximum sumcor peak height was 6.9 for SFS (indicated by squares along the top *x*-axis in Fig. 5F), but was 2.72 for SAM tones. Thus, the enhancement in envelope coding following NIHL was consistent for both SAM tones and for SFS, but the degree of enhancement may depend on the complexity of the stimulus.

Characteristics of the impaired AN fibers that showed a high degree of enhanced envelope coding were explored with all three envelope metrics; however, because results were consistent across metrics, results from only one metric are shown. The sumcor peak height metric was chosen because of its generality in application to arbitrary stimuli and the ability to compare envelope and fine-structure coding in single fibers from the same data set. Figure 6 shows that the sumcor and synchronization index metrics provide consistent representations of envelope coding for SAM tones. The BMLs computed from synchrony vs. level functions are plotted against the BMLs computed from sumcor peak height vs. level functions in Figure 6A for both normal and impaired AN fibers. Synchrony and sumcor BMLs showed a linear relationship, suggesting that the synchrony and sumcor peak height level functions reached a unique maximum at the same sound level. Both functions showed very similar non-monotonic envelope coding strength as a function of sound level.

Figure 6B shows sumcor peak height plotted versus synchronization index for both normal and noise-exposed fibers responding to SAM tones. All the fibers in Figure 6B had CFs in the range from 1 to 4 kHz. The monotonic relation between sumcor peak height and synchronization index was very similar for normal and impaired fibers. The distribution of impaired data points (circles) follows the same curve that defines the relation for normal-hearing fibers (crosses), with the impaired distribution simply shifted along the curve to higher values. The mean sumcor peak height was 1.93±0.39 (N=57) for impaired fibers and 1.55±0.23 (N=42) for normal fibers (p<0.005, unpaired t test), which indicates an average enhancement in envelope coding following NIHL (also see trend lines in Fig. 5). Figure 6B also clearly demonstrates that a subset of impaired fibers had stronger envelope coding than was observed in almost all of the normal-hearing fibers with similar CFs. In the normal-hearing population, only two (5%) AN fibers showed sumcor peak heights ≥2.0 (or equivalently synchronization index

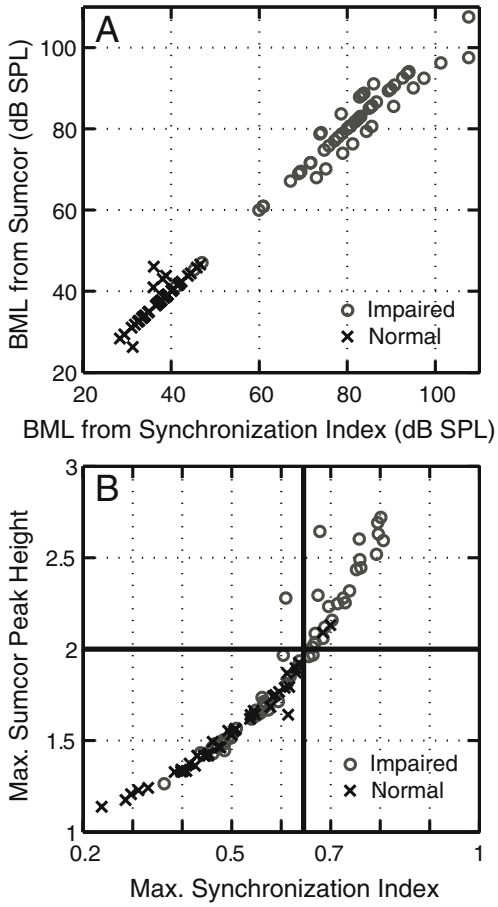

FIG. 6. Sumcor peak height and synchronization index provide consistent representations of strength of envelope coding. **A** Best modulation level (*BML*) computed from sumcor peak height vs. level functions is plotted against BML computed from synchronization index vs. level functions for individual fibers. **B** Maximum sumcor peak height is plotted against maximum synchronization index for individual fibers (*crosses*: normal hearing, *circles*: noise exposed). Almost all normal-hearing fibers had sumcor peak heights below 2.0 (*solid horizontal line*) and synchronization index values below 0.64 (*solid vertical line*). Noise-exposed fibers with maximum sumcor peak height ≥2.0 are referred to as having a "*high degree of enhanced envelope coding.*" All fibers are from the CF region of significant threshold shift (CFs=1–4 kHz) and data shown is for SAM tones.

R>0.64), whereas 26 (46%) of the noise-exposed fibers within the same CF region (1–4 kHz) showed sumcor peak heights >2.0. The maximum synchrony value of 0.64 for normal-hearing fibers is consistent with previous data from cats for SAM tones, where the maximum synchrony for CFs<5 kHz was 0.65 (Joris and Yin 1992). Based on these data, noise-exposed fibers with a sumcor peak height >2.0 were quantitatively classified as having a *high degree of enhanced envelope coding*. However, as stated earlier this subgroup of impaired fibers was not solely responsible for the elevation in mean sumcor peak height. For all normal and impaired fibers with sumcor peak height <2, mean sumcor peak heights were 1.51±0.21 (normal hearing), and 1.63±0.17 (impaired fibers). This difference in mean was statistically significant (p=0.01, unpaired t test). Further characterization of these fibers shown below was based on sumcor peak heights since Figure 6A, B demonstrate that sumcor peak height provides a similar characterization of the strength of envelope phase locking as the classic synchronization index. Although not shown, similar results were obtained using all three metrics.

A high degree of enhanced envelope coding was observed in fibers with high thresholds and very steep rate-level curves

To explore why a high degree of enhanced envelope coding was observed in some fibers, the relation between the strength of envelope coding and various AN response properties was characterized. Figure 7 compares sumcor peak height with two measures related to sound level: fiber threshold to CF tones (panel A) and BML for SAM tones (panel B). Fibers with a high degree of enhanced envelope coding are plotted above the solid horizontal line, which corresponds to a sumcor peak height value of 2.0. All but one noise-exposed fiber with a high degree of enhanced envelope coding had thresholds ranging from 63–90 dB SPL. In contrast, all but one noise-exposed fiber with sumcor peak heights below 2.0 had thresholds ranging from 20–74 dB SPL (lower-left quadrant). Thus, high threshold appears to be a necessary and sufficient condition for a high degree of enhanced envelope coding.

The sound level at which envelope coding was measured (BML) was also an important parameter associated with enhanced envelope coding. Figure 7B plots sumcor peak height as a function of the BML for SAM tones in individual fibers. All fibers with a high degree of enhanced envelope coding had very high BMLs (≥75 dB SPL); however, in contrast to fiber thresholds, not all fibers with very high BMLs had sumcor peak heights above 2.0 (lower right quadrant of Fig. 7B). These fibers with sumcor peak heights below 2.0 had pure tone thresholds lower than fibers which showed sumcor peak heights above 2.0.

The high sound levels (>75 dB SPL) at which most fibers showed a high degree of enhanced envelope coding could be associated with C2 responses, which typically have very steep rate-level functions, reduced spontaneous rate, and broadened tuning (Liberman and Dodds 1984a, b; Liberman and Kiang 1984; Heinz and Young 2004). Figure 8 shows sumcor peak height-level and CF-tone rate-level curves for one normal-hearing fiber (panel A) and two hearing-impaired fibers (panels B and C). The noise-exposed fiber with a high degree of enhanced envelope coding (sumcor peak height >2) showed a steep rate-level response (Fig. 8C), whereas the normal-hearing fiber (Fig. 8A)

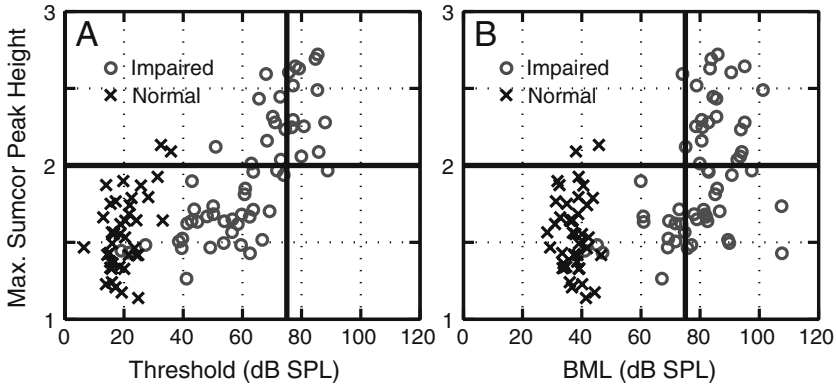

FIG. 7. Noise-exposed fibers with a high degree of enhancement in envelope coding always had very high thresholds and best modulation levels (*BMLs*); however, some fibers with very high BMLs had envelope coding within the normal range. Sumcor peak heights computed for SAM tones are plotted versus pure tone threshold (**A**) and best modulation level (**B**) for normal-hearing (*crosses*) and noise-exposed fibers (*circles*). *Vertical line* at 75 dB SPL marks the lower boundary of sound levels above which very steep rate-level functions were observed in some fibers. All CFs are between 1 and 4 kHz. Similar results were observed for single-formant stimuli.

and the noise-exposed fiber with sumcor peak height <2 showed shallower rate-level functions. Figure 9A plots sumcor peak height as a function of slope of the CF-tone rate-level function for individual fibers with CFs between 1–4 kHz. Strength of envelope coding increased roughly linearly with increasing rate-level slope for both normal and impaired populations. Most noise-exposed fibers with sumcor peak height above 2.0 had high rate-level slopes (above 5.0). All but one of the noise-exposed fibers with slopes above 10.0 showed very high sumcor peak heights (above 2.4). Most of the fibers with a high degree of enhanced envelope coding had CF rate-level functions with a very high threshold (>75 dB SPL) and a single very steep slope. These responses presumably arose from a C2 response in the absence of a C1 response, although this could not be confirmed with phase analyses of individual SAM components because the high threshold and high CFs (1–4 kHz) of these fibers precluded observation of the 180° phase shift often associated with the C1/C2 transition (Liberman and Kiang 1984). These fibers also had very high BMLs (>75 dB SPL, upper right quadrant of Fig. 7B), and thus envelope coding was measured in these fibers at very high sound levels. However, not all impaired fibers with very high BMLs (in the presumed C2 region) showed sumcor peak heights above 2.0. These fibers had relatively lower thresholds (Fig. 7A) and shallower rate-level slopes (Figs. 8B and 9A), which were presumably due to some residual C1-related responses (also see Fig. 8 of Heinz and Young 2004). Almost all noise-exposed fibers with slopes less than 5.0 had sumcor peak heights within the range of normal-hearing fibers (sumcor peak height <2.0). Thus, a high degree of enhanced envelope coding was associated with much steeper rate-level functions, presumably due to the invulnerable C2 response at high sound levels that remains even when the C1 response is mostly eliminated by NIHL.

The strength of envelope coding in AN fibers is inversely related to spontaneous rate (Joris and Yin

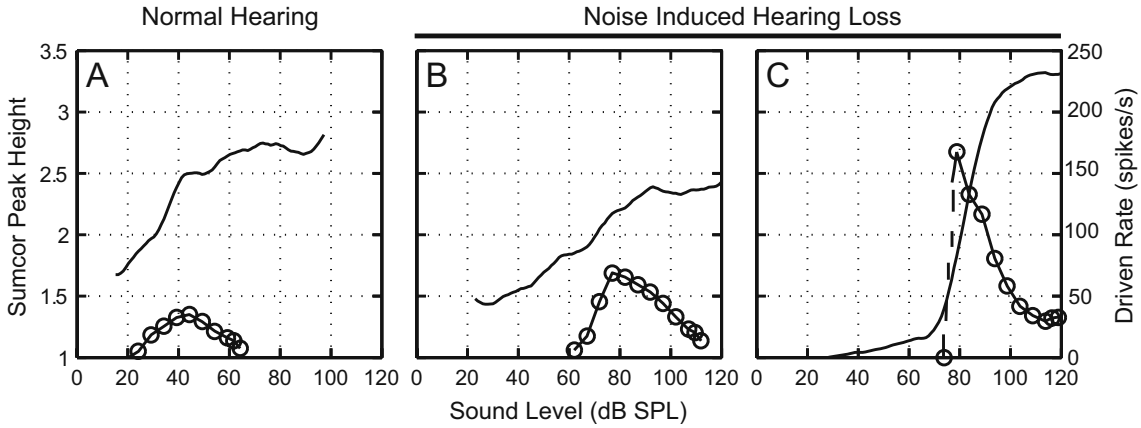

FIG. 8. Fibers with steeper CF-tone rate-level responses showed higher sumcor peak heights. **A** Normal-hearing fiber. **B** and **C** Noise-exposed fibers. The noise-exposed fiber in **C** showed a high degree of enhanced envelope coding (sumcor peak height ≥2.0) and steeper rate-level function. BF, threshold, Q_{10}, and SR of all three fibers are the same as in Figure 3.

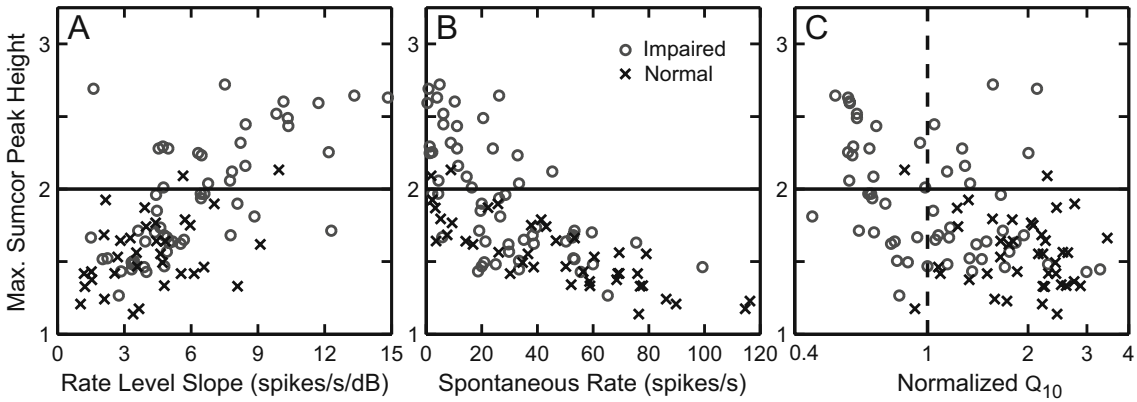

FIG. 9. A high degree of enhancement in envelope coding in noise-exposed fibers was most closely associated with steeper rate-level functions, but was also often associated with lower spontaneous rates and reduced frequency selectivity. Sumcor peak heights from individual normal-hearing (*crosses*) and noise-exposed (*circles*) fiber responses are plotted as a function of CF rate-level function slope (**A**), spontaneous rate (**B**), and normalized Q_{10} (**C**). Normalized Q_{10} values below 1 (*vertical dotted line*) indicate broader frequency selectivity than 95% of the normal-hearing population at the fiber's CF (see Fig. 2D). *Solid horizontal lines*: Sumcor peak height boundary used to classify fibers with a high degree of enhanced envelope coding. Only fibers from the CF region (1–4 kHz) of significant threshold shift are shown. Responses are to sinusoidally amplitude-modulated tones; however, similar trends were observed for single-formant stimuli.

1992). Thus, it is possible that enhanced envelope coding following NIHL could simply be due to the reduction in spontaneous rate that typically occurs following NIHL (Liberman and Dodds 1984a). Figure 9B plots sumcor peak height as a function of SR for normal and noise-exposed fibers with CFs between 1–4 kHz. Sumcor peak height decreased as SR increased for normal-hearing fibers, consistent with previous studies (Louage et al. 2004). The same trend was observed in the noise-exposed fibers, which tended to have lower SR on average than the normal-hearing fibers. Consistent with this trend, all noise-exposed fibers with sumcor peak heights above 2.0 had lower SRs (<~42 spikes/s). Most of the impaired fibers with SR<20 spikes/s showed a sumcor peak height above 2.0. However, impaired fibers with SRs between 20 and 40 spikes/s had sumcor peak heights ranging from 1.45 to 2.6. In addition, 80% of the normal-hearing fibers (and 29% of impaired fibers) with SR<20 spikes/s had sumcor peak heights <2.0. Thus, although lower SR was associated with a high degree of enhanced envelope coding, low SR was not a sufficient condition.

To explore the relation between reduced frequency selectivity and a high degree of enhanced envelope coding, sumcor peak heights were plotted against normalized Q_{10} values for normal and impaired fibers with CFs between 1 and 4 kHz (Fig. 9C). Normalized Q_{10} was computed for each AN fiber by dividing its Q_{10} by the Q_{10} corresponding to the 5th percentile of the normal-hearing population at the fiber's CF (Fig. 2B, D). Thus, normalized Q_{10} values below 1.0 correspond to significantly broadened tuning in noise-exposed fibers. In the normal-hearing population, sumcor peak height was independent of normalized Q_{10}. In contrast, many impaired fibers with sumcor peak heights above 2.0 had broadened tuning. These fibers also had steeper rate-level slopes (Fig. 9A) and lower SR (Fig. 9B). However, there were a number of noise-exposed fibers with broadened tuning and sumcor peak heights below 2.0. In addition, there were several impaired fibers with normalized Q_{10} between 1 and 2 (i.e., within the normal-hearing range) that had a high degree of enhanced envelope coding. Thus, although a high degree of enhanced envelope coding was typically associated with broadened tuning, this was not a sufficient condition.

The relative strength of fine structure to envelope coding was degraded following noise-induced hearing loss

Shuffled correlogram analyses allow both envelope and temporal fine-structure coding to be quantified from the same set of AN spike trains in response to any stimulus (Joris 2003). Sumcor and difcor peak heights quantify the strength of envelope and fine-structure coding, respectively, while the ratio of SCC (A+, A−) to SAC(A) quantifies the relative coding of envelope and fine structure (Louage et al. 2004). Figure 10A shows difcor peak heights plotted as a function of CF for both normal-hearing (crosses) and noise-exposed (circles) fiber responses to SAM tones. Each data point was computed at the sound level at which the difcor peak height was maximum, and thus represents the highest degree of fine-structure coding observed in each fiber responding to SAM tones. This was the same approach used to quantify the maximum degree of envelope coding based on the maximum sumcor (Fig. 5C). In all fibers (CF≤2.5 kHz), the difcor peak height versus level curve showed a unique maximum within ±5 dB of the BML based on the

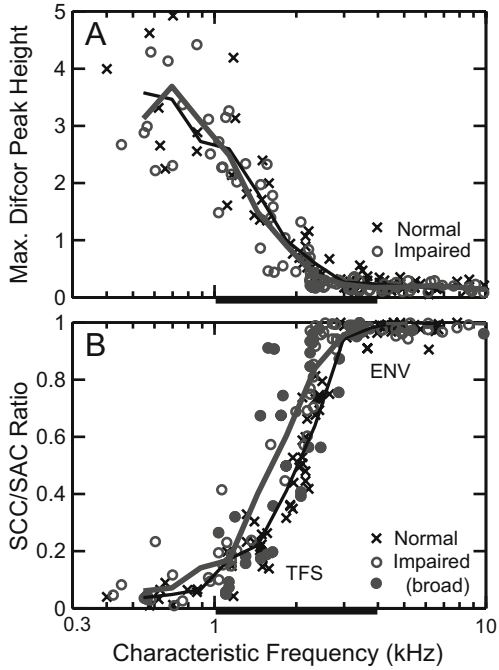

FIG. 10. The strength of temporal fine-structure (*TFS*) coding relative to envelope (*ENV*) coding was degraded in noise-exposed fibers, despite no degradation in the strength of TFS coding itself. **A** Maximum difcor peak heights quantify TFS coding for SAM tones, and are plotted as a function of characteristic frequency for normal (*crosses*) and noise-exposed fibers (*circles*). **B** The relative strength of TFS and ENV coding in individual-fiber responses is quantified as the ratio of SCC(A+, A−) to SAC(A) at zero delay, where a ratio value near 0 represents primarily TFS coding and a value near 1 represents mainly ENV coding. *Filled circles* represent fibers with broad tuning (normalized Q_{10}<1.0). *Solid lines* (*thin*: normal hearing, *thick*: noise exposed) are triangular weighted averages (as in Fig. 5). *Thick horizontal bar*: CF region (1–4 kHz) of significant threshold shifts.

sumcor. Difcor peak height decreased with increasing CF (Fig. 10A), similar to data from cats (Louage et al. 2004). The same pattern was observed for noise-exposed fibers, with very similar distributions and trend lines between the normal and impaired populations. Thus, the strength of fine-structure coding in individual AN fibers responding to SAM tones was not affected by noise-induced hearing loss.

The relative strength of fine-structure and envelope coding in individual AN fibers was quantified with the ratio of SCC(A+, A−) to SAC(A), which was computed at zero delay and at the sumcor BML (Fig. 10B). When fine structure dominates the response, the value of SCC(A+, A−) at zero delay is low and the value of SAC(A) is high, and thus the ratio is near zero. In contrast, when envelope dominates the response, inverting the stimulus polarity has little effect and the value of SCC(A+, A−) is similar to SAC(A), i.e., the ratio is near one. The dependence of the SCC/SAC ratio on CF is sigmoidal in shape for normal-hearing fibers and quantifies the transition from fine structure dominance at low CFs to envelope dominance at high CFs, consistent with previous studies (Louage et al. 2004). The transition from 0 to 1 for the chinchilla normal-hearing population occurred over the CF range between 1 to 3 kHz, which is slightly lower than the 2–4 kHz range for cats (Louage et al. 2004). A similar sigmoidal dependence on CF was observed in the noise-exposed population (circles). However, the transition in the noise-exposed population occurred at lower CFs (0.5 to 2 kHz) than in the normal-hearing population. Thus, there was a reduced CF range over which AN fiber responses were dominated by fine structure following NIHL. For a given CF in the transition region, the relative strength of envelope to fine-structure coding was higher in noise-exposed fibers than in normal-hearing fibers. This effect occurred whether or not the noise-exposed fiber had broadened tuning (filled circles) or tuning within normal limits (open circles), and thus does not appear to depend on reduced frequency selectivity. Similar trends were observed for single-formant stimuli. Thus, a relative fine-structure deficit was observed in the noise-exposed population in that the fine-structure-dominated CF region was reduced, although the strength of fine-structure coding itself was not degraded.

DISCUSSION

The fundamental ability of AN fibers to encode temporal envelope and fine structure was not degraded with noise-induced hearing loss

There are inconsistent data regarding the effects of SNHL on the strength of AN phase locking to pure tones. One study showed degradation in phase locking following selective outer hair cell damage induced by kanamycin in chinchillas (Woolf et al. 1981). However, the majority of studies report no degradation in pure tone phase locking following SNHL, e.g., in guinea pigs following kanamycin (Harrison and Evans 1979) and in cats following acoustic trauma (Miller et al. 1997; Heinz and Young, personal communication). The present data extend these studies to quantify phase locking to both stimulus fine structure and envelope for more complex stimuli, specifically narrowband-modulated stimuli. It is important to consider phase locking to both fine structure and envelope since several additional mechanisms appear to limit envelope coding beyond those that limit fine-structure coding (Joris and Yin 1992).

The present data showed that the strength of phase locking to fine structure of SAM tones was similar between normal-hearing and noise-exposed fibers. In contrast, envelope phase locking was enhanced on average following NIHL, particularly for fibers with

moderate–severe threshold shifts. The degree of enhancement was dependent on stimulus complexity, with greater enhancement for SFS than for SAM tones. The lack of degradation in envelope coding is consistent with perceptual data showing no degradation in the abilities of hearing-impaired listeners in amplitude-modulation detection (Bacon and Gleitman 1992; Moore and Glasberg 2001) and envelope-vocoded speech perception in quiet (Baskent 2006; Lorenzi et al. 2006). Beyond the lack of degradation, the observed enhancement in envelope coding is consistent with data from several gap-detection and modulation-detection studies (Glasberg and Moore 1992; Moore et al. 1996; Fullgrabe et al. 2003). These perceptual results were hypothesized to result from loudness-recruitment effects associated with the loss of cochlear compression due to outer hair cell damage; however, the present data suggest reduced compression is not the most significant physiological factor producing enhanced envelope coding, as discussed below.

Physiological sources of enhanced envelope coding

Fibers with a high degree of enhanced envelope coding typically had high thresholds, very steep rate-level functions, lower SR, and broadened tuning. However, high thresholds and very steep rate-level functions were the only primary factors (i.e., both necessary and sufficient) in producing a high degree of enhanced envelope coding. Lower SR is associated with better envelope coding (Louage et al. 2004); however, this consequence of SNHL (Liberman and Dodds 1984a) was not the primary cause of enhanced envelope coding since similar SRs in normal-hearing fibers did not produce sumcor peak heights >2.0 (Fig. 9B). Broadened tuning was also not a primary factor, as many noise-exposed fibers with broadened tuning (Fig. 9C) did not show a high degree of enhanced envelope coding. Thus, low SR and reduced frequency selectivity appear to be mainly secondary properties associated with, but not directly responsible for, enhanced envelope coding.

The very steep rate-level slopes that occur with moderate–severe threshold elevation likely represent C2 responses in the absence of C1 responses. C2 responses are invulnerable to severe cochlear damage even when the C1 responses that dominate at low–moderate sound levels are completely eliminated (Liberman and Kiang 1984; Sewell 1984; Heinz and Young 2004). Although these high-level C2 effects are often ignored for normal hearing, these effects are significant for speech perception by listeners with SNHL since these are the sound levels at which hearing aids operate (Zilany and Bruce 2007). In previous studies with noise-exposed animals, cochlear regions showing only C2 responses were associated with significant damage to the tallest row of inner hair cell stereocilia and all rows of outer hair cell stereocilia (Liberman and Kiang 1984). In cases without significant inner hair cell damage, C1 responses were typically present and very steep rate-level functions were not observed. Thus, the high degree of enhanced envelope coding associated with very steep rate-level functions in the present study likely resulted primarily from significant inner hair cell stereocilia damage.

Although reduced cochlear compression has been suggested to produce enhanced envelope coding (Glasberg and Moore 1992; Moore et al. 1996), the influence of basilar-membrane compression on AN rate-level functions is limited by their restricted dynamic range (Sachs and Abbas 1974) and the confounding influence of inner hair cell damage (Heinz and Young 2004). Nonetheless, the present data indicated that envelope coding was on average enhanced following NIHL, even when fibers showing a high degree of enhancement were excluded. Thus, envelope coding appears to be mildly enhanced for mild–moderate hearing loss (presumably due to reduced cochlear compression), but to be greatly enhanced for moderate–severe hearing loss (due to very steep C2 responses in the absence of C1 responses). These data suggest that both inner and outer hair cell damage can affect temporal envelope coding, but that strong phase locking remains even with significant inner and/or outer hair cell stereocilia damage.

"Enhanced" envelope coding can be detrimental to hearing-impaired listeners

Enhanced envelope coding has been hypothesized to underlie improved modulation detection in some hearing-impaired listeners because amplitude fluctuations would be magnified and thus be more prominent perceptually (Moore et al. 1996; Fullgrabe et al. 2003). However, this apparent perceptual benefit has important implications for the difficulties faced by hearing-impaired listeners in real-world environments (e.g., in temporally fluctuating background noises such as competing talkers). Normal-hearing listeners show better speech intelligibility when background noise has temporal fluctuations, whereas hearing-impaired listeners typically fail to benefit from fluctuations in background noise (Duquesnoy 1983; Festen and Plomp 1990). It is possible that magnified masker fluctuations due to enhanced envelope coding could be a distraction that would reduce speech intelligibility. This idea is consistent with simulations of the effects of loudness recruitment with normal-hearing listeners, which showed that

amplitude expansion reduced speech intelligibility, particularly in fluctuating background noises (Villchur 1977; Moore and Glasberg 1993; Moore et al. 1995). Enhanced envelope coding is also likely to contribute to reduced ability of hearing-impaired listeners to detect temporal gaps between narrowband noises (Fitzgibbons and Wightman 1982; Glasberg et al. 1987; Glasberg and Moore 1992). Thus, enhanced envelope coding following SNHL can have detrimental effects on the ability of hearing-impaired listeners to listen in the presence of complex background noises, which are the conditions for which hearing aids currently are least effective in restoring normal perception (Moore et al. 1999).

Enhanced envelope coding produces a "relative" fine-structure coding deficit

Recent perceptual studies suggest that hearing-impaired listeners have reduced ability to use fine-structure cues for both speech and pitch perception (Buss et al. 2004; Lorenzi et al. 2006; Hopkins and Moore 2007; Hopkins et al. 2008); however, the physiological correlates of this fine-structure deficit continue to be debated (Moore and Carlyon 2005; Moore 2008). Although the fundamental ability of AN fibers to phase lock to fine structure was not degraded following SNHL (Fig. 10A), the present data suggest that enhanced envelope coding shifted the transition between primarily fine structure and envelope coding to lower CFs following SNHL (Fig. 10B). Thus, preferential phase locking of noise-exposed fibers to envelope can be considered as a deficit in the relative strength of fine-structure coding in these fibers. This 'relative' deficit was most prominent for CFs between 1 and 3 kHz. Thus, this fine-structure deficit may be particularly relevant for speech, for which much information is provided in the 1–3 kHz frequency range (French and Steinberg 1947; Ardoint and Lorenzi 2010). This deficit also occurred whether or not noise-exposed fibers had broadened tuning, consistent with recent perceptual evidence that reduced ability to use fine-structure cues is not correlated with reduced frequency selectivity (Santurette and Dau 2007; Lorenzi et al. 2009; Strelcyk and Dau 2009). For pitch perception, reduced frequency selectivity is often thought to cause listeners with SNHL to rely more on the less salient envelope cues created by unresolved harmonics than the more salient fine-structure cues associated with resolved harmonics (Moore and Carlyon 2005). The present data suggest that enhanced envelope coding and the associated relative fine-structure deficit is an additional factor that may contribute to listeners with SNHL relying more on the less salient envelope cues for pitch perception. Thus, it is likely to be important to consider the relative coding of fine structure and envelope, not just fine structure alone, in interpreting perceptual deficits in using fine-structure cues, particularly for complex stimuli and listening environments.

Other effects of SNHL on temporal coding

The stimuli and analyses in the present study did not address all effects of SNHL on temporal coding that may be perceptually relevant. Narrowband amplitude-modulated stimuli were used to characterize the fundamental ability of AN fibers to phase lock to envelope and fine structure. However, changes in the specific fine-structure frequency components to which noise-exposed AN fibers phase lock (e.g., abnormal upward spread of first-formant components, Miller et al. 1997) were not addressed, but may contribute to perceptual deficits in using fine-structure cues with broadband stimuli. Also, reduced traveling-wave delays between cochlear locations and increased across-CF correlation in fine structure and envelope responses occur following SNHL (Heinz et al. 2010). These across-fiber effects degrade spatio-temporal coding, which has been hypothesized to be perceptually relevant for both speech (Shamma 1985; Heinz 2007) and pitch perception (Loeb et al. 1983; Cedolin and Delgutte 2007).

ACKNOWLEDGMENTS

The project described was supported by Award Numbers R03DC007348 and R01DC009838 from the National Institute on Deafness and Other Communication Disorders. The content is solely the responsibility of the authors and does not necessarily represent the official views of the National Institute on Deafness and Other Communication Disorders or the National Institutes of Health. Support from the American Hearing Research Foundation also contributed to this work. The authors thank Jayaganesh Swaminathan and Ananthakrishna Chintanpalli for help with data collection. Elizabeth Strickland and Jonathan Boley provided valuable comments on an earlier version of this manuscript.

REFERENCES

Ardoint M, Lorenzi C (2010) Effects of lowpass and highpass filtering on the intelligibility of speech based on temporal fine structure or envelope cues. Hear Res 260:89–95

Bacon SP, Gleitman RM (1992) Modulation detection in subjects with relatively flat hearing losses. J Speech Hear Res 35:642–653

Baskent D (2006) Speech recognition in normal hearing and sensorineural hearing loss as a function of the number of spectral channels. J Acoust Soc Am 120:2908–2925

Bruce IC, Sachs MB, Young ED (2003) An auditory-periphery model of the effects of acoustic trauma on auditory nerve responses. J Acoust Soc Am 113:369–388

Buss E, Hall JW 3rd, Grose JH (2004) Temporal fine-structure cues to speech and pure tone modulation in observers with sensorineural hearing loss. Ear Hear 25:242–250

CEDOLIN L, DELGUTTE B (2007) Spatio-temporal representation of the pitch of complex tones in the auditory nerve. In: Kollmeier B, Klump G, Hohmann V, Langemann U, Mauermann M, Uppenkamp S, Verhey J (eds) Hearing—from sensory processing to perception. Springer, Berlin, pp 61–70

CHINTANPALLI A, HEINZ MG (2007) The effect of auditory-nerve response variability on estimates of tuning curves. J Acoust Soc Am 122:EL203–EL209

DUQUESNOY AJ (1983) Effect of a single interfering noise or speech source upon the binaural sentence intelligibility of aged persons. J Acoust Soc Am 74:739–743

FESTEN JM, PLOMP R (1990) Effects of fluctuating noise and interfering speech on the speech-reception threshold for impaired and normal hearing. J Acoust Soc Am 88:1725–1736

FITZGIBBONS PJ, WIGHTMAN FL (1982) Gap detection in normal and hearing-impaired listeners. J Acoust Soc Am 72:761–765

FRENCH NR, STEINBERG JC (1947) Factors governing the intelligitility of speech sounds. J Acoust Soc Am 19:90–119

FULLGRABE C, MEYER B, LORENZI C (2003) Effect of cochlear damage on the detection of complex temporal envelopes. Hear Res 178: 35–43

GLASBERG BR, MOORE BCJ (1992) Effects of envelope fluctuations on gap detection. Hear Res 64:81–92

GLASBERG BR, MOORE BCJ, BACON SP (1987) Gap detection and masking in hearing-impaired and normal-hearing subjects. J Acoust Soc Am 81:1546–1556

GOLDBERG JM, BROWN PB (1969) Response of binaural neurons of dog superior olivary complex to dichotic tonal stimuli: some physiological mechanisms of sound localization. J Neurophysiol 32:613–636

GUINAN JJ JR, PEAKE WT (1967) Middle-ear characteristics of anesthetized cats. J Acoust Soc Am 41:1237–1261

HARRISON RV, EVANS EF (1979) Some aspects of temporal coding by single cochlear fibres from regions of cochlear hair cell degeneration in the guinea pig. Arch Otorhinolaryngol 224:71–78

HEINZ MG (2007) Spatiotemporal encoding of vowels in noise studied with the responses of individual auditory nerve fibers. In: Kollmeier B, Klump G, Hohmann V, Langemann U, Mauermann M, Uppenkamp S, Verhey J (eds) Hearing – from sensory processing to perception. Springer-Verlag, Berlin, pp 107–115

HEINZ MG, SWAMINATHAN J (2009) Quantifying envelope and fine-structure coding in auditory nerve responses to chimaeric speech. J Assoc Res Otolaryngol 10:407–423

HEINZ MG, YOUNG ED (2004) Response growth with sound level in auditory-nerve fibers after noise-induced hearing loss. J Neurophysiol 91:784–795

HEINZ MG, ISSA JB, YOUNG ED (2005) Auditory-nerve rate responses are inconsistent with common hypotheses for the neural correlates of loudness recruitment. J Assoc Res Otolaryngol 6:91–105

HEINZ MG, SWAMINATHAN J, BOLEY JD, KALE S (2010) Across-fiber coding of temporal fine-structure: effects of noise-induced hearing loss on auditory-nerve responses. In: Lopez-Poveda EA, Palmer AR, Meddis R (eds) The neurophysiological bases of auditory perception. Springer, New York, pp 621–630

HOPKINS K, MOORE BCJ (2007) Moderate cochlear hearing loss leads to a reduced ability to use temporal fine structure information. J Acoust Soc Am 122:1055–1068

HOPKINS K, MOORE BCJ, STONE MA (2008) Effects of moderate cochlear hearing loss on the ability to benefit from temporal fine structure information in speech. J Acoust Soc Am 123:1140–1153

JOHNSON DH (1980) The relationship between spike rate and synchrony in responses of auditory-nerve fibers to single tones. J Acoust Soc Am 68:1115–1122

JORIS PX (2003) Interaural time sensitivity dominated by cochlea-induced envelope patterns. J Neurosci 23:6345–6350

JORIS PX, YIN TC (1992) Responses to amplitude-modulated tones in the auditory nerve of the cat. J Acoust Soc Am 91:215–232

KIANG NYS, WATANABE T, THOMAS EC, CLARK LF (1965) Discharge patterns of single fibers in the cat's auditory nerve. MIT, Cambridge

KIANG NYS, MOXON EC, LEVINE RA (1970) Auditory-nerve activity in cats with normal and abnormal cochleas. In: Wolstenholme GEW, Knight T (eds) Sensorineural hearing loss. Churchill, London, pp 241–273

LIBERMAN MC (1984) Single-neuron labeling and chronic cochlear pathology. I. Threshold shift and characteristic-frequency shift. Hear Res 16:33–41

LIBERMAN MC, DODDS LW (1984a) Single-neuron labeling and chronic cochlear pathology. II. Stereocilia damage and alterations of spontaneous discharge rates. Hear Res 16:43–53

LIBERMAN MC, DODDS LW (1984b) Single-neuron labeling and chronic cochlear pathology. III. Stereocilia damage and alterations of threshold tuning curves. Hear Res 16:55–74

LIBERMAN MC, KIANG NYS (1984) Single-neuron labeling and chronic cochlear pathology. IV. Stereocilia damage and alterations in rate- and phase-level functions. Hear Res 16:75–90

LOEB GE, WHITE MW, MERZENICH MM (1983) Spatial cross-correlation—a proposed mechanism for acoustic pitch perception. Biol Cybern 47:149–163

LORENZI C, GILBERT G, CARN H, GARNIER S, MOORE BCJ (2006) Speech perception problems of the hearing impaired reflect inability to use temporal fine structure. Proc Natl Acad Sci U S A 103: 18866–18869

LORENZI C, DEBRUILLE L, GARNIER S, FLEURIOT P, MOORE BCJ (2009) Abnormal processing of temporal fine structure in speech for frequencies where absolute thresholds are normal. J Acoust Soc Am 125:27–30

LOUAGE DH, VAN DER HEIJDEN M, JORIS PX (2004) Temporal properties of responses to broadband noise in the auditory nerve. J Neurophysiol 91:2051–2065

MARDIA KV, JUPP PE (2000) Directional statistics. Wiley, New York

MILLER RL, SCHILLING JR, FRANCK KR, YOUNG ED (1997) Effects of acoustic trauma on the representation of the vowel /ε/ in cat auditory nerve fibers. J Acoust Soc Am 101:3602–3616

MOORE BCJ (2008) The role of temporal fine structure processing in pitch perception, masking, and speech perception for normal-hearing and hearing-impaired people. J Assoc Res Otolaryngol 9:399–406

MOORE BCJ, CARLYON RP (2005) Perception of pitch by people with cochlear hearing loss and by cochlear implant users. In: Plack CJ, Oxenham AJ, Fay RR, Popper AN (eds) Pitch neural coding and perception. Springer, New York

MOORE BCJ, GLASBERG BR (1993) Simulation of the effects of loudness recruitment and threshold elevation on the intelligibility of speech in quiet and in a background of speech. J Acoust Soc Am 94:2050–2062

MOORE BCJ, GLASBERG BR (2001) Temporal modulation transfer functions obtained using sinusoidal carriers with normally hearing and hearing-impaired listeners. J Acoust Soc Am 110:1067–1073

MOORE BCJ, GLASBERG BR, VICKERS DA (1995) Simulation of the effects of loudness recruitment on the intelligibility of speech in noise. Br J Audiol 29:131–143

MOORE BCJ, WOJTCZAK M, VICKERS DA (1996) Effect of loudness recruitment on the perception of amplitude modulation. J Acoust Soc Am 100:481–489

MOORE BCJ, PETERS RW, STONE MA (1999) Benefits of linear amplification and multichannel compression for speech comprehension in backgrounds with spectral and temporal dips. J Acoust Soc Am 105:400–411

NGAN EM, MAY BJ (2001) Relationship between the auditory brainstem response and auditory nerve thresholds in cats with hearing loss. Hear Res 156:44–52

Qin MK, Oxenham AJ (2003) Effects of simulated cochlear-implant processing on speech reception in fluctuating maskers. J Acoust Soc Am 114:446–454

Sachs MB, Abbas PJ (1974) Rate versus level functions for auditory-nerve fibers in cats: tone-burst stimuli. J Acoust Soc Am 56:1835–1847

Santurette S, Dau T (2007) Binaural pitch perception in normal-hearing and hearing-impaired listeners. Hear Res 223:29–47

Sek A, Moore BCJ (2006) Perception of amplitude modulation by hearing-impaired listeners: the audibility of component modulation and detection of phase change in three-component modulators. J Acoust Soc Am 119:507–514

Sewell WF (1984) Furosemide selectively reduces one component in rate-level functions from auditory-nerve fibers. Hear Res 15:69–72

Shamma SA (1985) Speech processing in the auditory system. I: the representation of speech sounds in the responses of the auditory nerve. J Acoust Soc Am 78:1612–1621

Shannon RV, Zeng FG, Kamath V, Wygonski J, Ekelid M (1995) Speech recognition with primarily temporal cues. Science 270:303–304

Strelcyk O, Dau T (2009) Relations between frequency selectivity, temporal fine-structure processing, and speech reception in impaired hearing. J Acoust Soc Am 125:3328–3345

Temchin AN, Rich NC, Ruggero MA (2008) Threshold tuning curves of chinchilla auditory nerve fibers. II. Dependence on spontaneous activity and relation to cochlear nonlinearity. J Neurophysiol 100:2899–2906

Villchur E (1977) Electronic models to simulate the effect of sensory distortions on speech perception by the deaf. J Acoust Soc Am 62:665–674

Wang X, Sachs MB (1993) Neural encoding of single-formant stimuli in the cat. I. Responses of auditory nerve fibers. J Neurophysiol 70:1054–1075

Woolf NK, Ryan AF, Bone RC (1981) Neural phase-locking properties in the absence of cochlear outer hair cells. Hear Res 4:335–346

Zeng FG, Nie K, Stickney GS, Kong YY, Vongphoe M, Bhargave A, Wei C, Cao K (2005) Speech recognition with amplitude and frequency modulations. Proc Natl Acad Sci U S A 102:2293–2298

Zilany MSA, Bruce IC (2007) Representation of the vowel /ε/ in normal and impaired auditory nerve fibers: model predictions of responses in cats. J Acoust Soc Am 122:402–417